Evaluation of modeled surface ozone biases as a function of cloud cover fraction

Hyun Cheol Kim[1,2], Pius Lee[1], Fong Ngan[1,2], Youhua Tang[1,2], Hye Lim Yoo[1,2], and Li Pan[1,2]

[1] NOAA/Air Resources Laboratory, College Park, MD

[2] UMD/Cooperative Institute for Climate and Satellites, College Park, MD

ABSTRACT

A regional air-quality forecast system's model of surface ozone variability based on cloud coverage is evaluated using satellite-observed cloud fraction (CF) information and a surface air-quality monitoring system. We compared CF and daily maximum ozone from the National Oceanic and Atmospheric Administration's National Air Quality Forecast Capability (NOAA NAQFC) with CFs from the Moderate Resolution Imaging Spectroradiometer (MODIS) and the U.S. Environmental Protection Agency's AirNow surface ozone measurements during May to October, 2014. We found that observed surface ozone shows a negative correlation with the MODIS CFs, showing around 1 ppb decrease for 10% MODIS CF change over the Contiguous United States, while the correlation of modeled surface ozone with the model CFs is much weaker, showing only -0.5 ppb per 10% NAQFC CF change. Further, daytime CF differences between MODIS and NAQFC are correlated with modeled surface-ozone biases between AirNow and NAQFC, showing -1.05 ppb per 10% CF change, implying that spatial- and temporal-misplacement of the modeled cloud field might have biased modeled surface ozone-level. Current NAQFC cloud fields seem to have less CFs compared to MODIS cloud fields (mean NAQFC CF = 0.38 and mean MODIS CF = 0.55), contributing up to 35% of surface-ozone bias in the current NAQFC system.

1. INTRODUCTION

Ground-level ozone is a secondary pollutant resulting from photochemical reactions between oxides of nitrogen (NO_x) and volatile organic compounds (VOC) in the presence of solar radiation. While local ozone production is affected by numerous factors, including precursor emissions and meteorological conditions such as temperature and local circulation, ozone photochemistry is photon-limited, and net ozone production shows a direct relationship with changes in UV actinic flux resulting from clouds and aerosols (Dickerson et al., 1997; He and Carmichael, 1999; Jacobson, 1998; Monks et al., 2004). For instance, Lefer et al. (2003) showed that without sufficient UV radiation, ozone production in Houston is limited regardless of local circulation patterns or emission sources. Studies in the urban cities of Los Angeles, California (Jacobson, 1998) and Mexico City (Castro et al., 2001; Raga, Castro et al., 2001), also showed that surface ozone varies from 5% to 30% due to light-absorbing aerosols. Model studies have shown that surface ozone is affected by cloud fields (Voulgarakis et al., 2009; Wild et al., 2000) or strongly scattering aerosols (Dickerson et al., 1997; He and Carmichael, 1999).

Since clouds play a critical role in the radiative balance of the Earth, their impact and models' capabilities to simulate clouds have been repeatedly tested from global and climate

perspectives (Bergman and Salby, 1996; Eastman and Warren, 2013; Stephens, 2005). Clouds also play an important role in regional air quality, impacting both surface ozone and particulate matter by regulating photochemical reaction rates, heterogeneous chemistry, and the evolution and partitioning of particulate matter. These impacts, however, still have high measurement uncertainties and are not well quantified. While reliable estimates of photolysis rates are essential for reducing the uncertainty in air-quality modeling, most current models use highly parameterized methods to estimate photolysis rates. Pour-Biazar et al. (2007) argued that the uncertainties in estimation of cloud transmissivity and errors in the placement of clouds' location and time could be an important source of uncertainties in simulations of surface ozone, demonstrating during the Texas Air Quality Study campaign that surface-ozone modeling can be improved by adjusting photolysis rates based on the Geostationary Operational Environmental Satellite cloud product. They also stated that the cloud-prediction problem is particularly frustrating when modeling air quality in State Implementation Plans if they are not able to reproduce satellite-observed cloud fields in a model.

In order to reduce computational cost, most regional air-quality models, including the US Environmental Protection Agency (EPA) Community Multi-scale Air Quality model (CMAQ), use a two-step approach for calculating photolysis rates (Byun and Schere, 2006). In preprocessing, the clear-sky photolysis rates for a range of latitudes, altitudes, and solar zenith angles are first computed using a radiative transfer module (Madronich, 1987). Then, within the chemical-transport model, the tabular photolysis rates are interpolated for each location and then adjusted using fractional cloud-coverage information. Since most early meteorological models did not generate the full suite of specific cloud and moisture fields required as input for the chemical-transport model, regional air-quality models were designed to diagnose some additional cloud-related fields from meteorological state variables for use in the chemical-transport model. The Meteorology-Chemistry Interface Processor (MCIP), CMAQ's preprocessor, diagnoses for each horizontal grid cell the cloud coverage, cloud base and top, and the average liquid water content in the cloud using a series of simple algorithms based on a relative-humidity threshold (Otte and Pleim, 2010). For example, in CMAQ modules the photolysis rates below clouds are calculated as:

$$J_{below} = J_{clear}[1 + f_c(1.6 \cdot tr_c \cos(\theta) - 1)] \quad (1)$$

where tr_c is cloud transmissivity, f_c is the cloud fraction for a grid cell, and Θ is the solar zenith angle. Cloud fraction is estimated using relative humidity (RH) and critical RH (Byun and Ching, 1999). Cloud fraction (f_c^k) above the boundary layer is:

$$f_c^k = \left[\frac{RH^k - RH_c}{1 - RH_c}\right]^2 \quad (2)$$

where RH^k is the relative humidity at vertical model layer k and RH_c is the critical relative humidity defined as $RH_c = 1 - 2\sigma_c(1 - \sigma_c)[1 + 1.732(\sigma_c - 0.5)]$ and $\sigma_c = p^k/p^{k_{PBL}}$ (Geleyn et al., 1982).

Within the convective boundary layer when $RH > RH_c$,

$$f_c^k = 0.34\frac{RH^k - RH_c}{1 - RH_c} \quad (3)$$

(Schumann, 1989; Wyngaard and Brost, 1984). See line 131-177 of bcldprc_ak.f90 for MCIP v3.6.

Although fractional cloud coverage (i.e., cloud fraction) thus plays a crucial role in determining the final values for photolysis rate, it is not a well-defined physical state variable and is mostly threshold-specific for each retrieval algorithm. One may notice that there are two possible uncertainties in modeling cloud fraction: (1) the model's capability to generate the proper amount of cloud fields, both in their displacement and timing; and (2) conceptual consistency in definitions of cloud fraction between model and observation (i.e., from satellite). In this study, we present efforts to evaluate the cloud-coverage information used in a regional air-quality model through satellite-based cloud fraction information and surface-monitored ozone observations. In the second section, we introduce the observational and modeling data used in this analysis, and results are discussed in Section 3. General performance of the Contiguous United States (CONUS)-scale air-quality forecast system and possible overestimation of surface-ozone levels due to uncertainty in cloud fractions will be also discussed.

2. DATA AND METHOD

MODIS: The Moderate Resolution Imaging Spectroradiometer (MODIS) cloud level 2 product (MOD06_L2 and MYD06_L2, http://modis-atmos.gsfc.nasa.gov/MOD06_L2/index.html) is used for daily cloud-coverage information for each surface-monitoring site. We have retrieved 5-km cloud fraction data, which is based on MOD35_L2 cloud-mask information with 1km and 250m (nadir) spatial resolution. Brightness temperatures (BT) from multiple channels and their differences (BTD) are used in cloud-masking algorithms, as described in the MODIS cloud-mask product (MOD35_L2) user guide (http://modis-atmos.gsfc.nasa.gov/_docs/CMUSERSGUIDE.pdf). For example, daytime land-cloud maskings are determined using BTs and BTDs from 1.38-, 3.7-, 3.9-, 6.7-, 8-, 11-, 12-, and 13.9- μm channels. Only data from local afternoon time (~1:30 pm), when ground-level data show high ozone-production efficiency, are used in the analysis.

AirNow: Real-time ozone measurements across the CONUS are provided by the EPA through the AirNow network (http://www.epa.gov/airnow). From more than 1000 Air Quality System (AQS) sites throughout the CONUS, hourly surface ozone data is obtained, and a daily maximum eight-hour moving averaged ozone (MDA8 ozone) value is calculated for each site.

NAQFC: The U.S. National Air Quality Forecast Capability (NAQFC) provides daily, ground-level ozone predictions using the Weather Forecasting and Research non-hydrostatic mesoscale model (WRF-NMM) and CMAQ framework across the CONUS with 12-km resolution domain (Chai et al., 2013; Eder et al., 2009). In our analysis, we used the experimental version of NAQFC, which uses WRF-NMM with B-grid (NMMB) as a meteorological driver and the CB05 chemical mechanism. Meteorological data is processed using the PREMAQ, which is a special version of MCIP designed for the NAQFC system. While NAQFC has shown a tendency to overpredict MDA8 ozone (Chai et al., 2013), recent updates to model processes and emission have reduced its bias. The "CFRAC" variable from METCRO2D output files are used for cloud fraction.

METHOD: For each EPA monitoring site and the corresponding model cells, we have calculated a daily maximum of eight-hour, forward-moving, averaged concentrations. For the same

115 locations, we also calculated daytime (~1:30pm local time) cloud fractions from the model and
116 from satellite data. MODIS cloud fractions are regridded into 12-km domain grid cells using a
117 conservative regridding method (Kim et al., 2013). For consistent comparisons, only valid
118 observational data are used, those with corresponding times and locations. We have
119 investigated the six-month summer ozone season (May-October, 2014) and results are
120 consistent for each month.

121 ## 3. RESULTS AND DISCUSSION

122 General distributions of daily and monthly daytime cloud fractions from the model and from
123 satellite are compared. Figure 1 shows the distribution of cloud fractions retrieved from NAQFC
124 and MODIS cloud products (MOD06 level2) for one day (Aug. 2, 2014) in the upper panels; and
125 the figure shows a one-month average (Aug. 2014) in the lower panels. The August 2 plot is
126 overlaid with a NCEP surface-analysis chart to show its association with general features of the
127 synoptic weather pattern. It is obvious that both model and satellite correctly display the
128 general features of cloud coverage associated with the synoptic frontal activities. However,
129 there is a serious discrepancy in their quantity; in most cases the amount of cloud fraction used
130 in the model is smaller than the cloud fraction retrieved from the MODIS cloud product. For
131 August 2014, monthly means of daytime cloud-fractions from NAQFC and MODIS are 0.38 and
132 0.55, respectively.

133 This discrepancy becomes even more evident from the histogram distribution. In Figure 2, we
134 present histogram distributions of cloud fractions from NAQFC and from MODIS during August
135 2014 for each 0.1 cloud-fraction bin. Occurrence frequency is shown on the y-axis, so the sum of
136 total frequency makes 100%. In the NAQFC model, lower cloud-fraction numbers are more
137 dominant, with the highest frequency between 0.2 and 0.3, showing very low frequency of high
138 cloud fractions. On the other hand, the MODIS cloud fraction is quite different, showing more of
139 a bimodal distribution. Frequencies for clear sky are similar between the model and satellite,
140 around 12–13%, but the satellite cloud frequency is much lower in the 0.1–0.5 range and higher
141 above 0.6.

142 The reason for this discrepancy between the model and MODIS is not clear and requires future
143 investigation. As mentioned previously, this might be a characteristic of the meteorological
144 model or it could be a conceptual difference in cloud fraction between model and satellite. As
145 cloud-fraction field is a diagnosed variable in PREMAQ, which uses a certain threshold of liquid-
146 water content or relative humidity to model the existence of clouds, it may differ from the
147 satellite's measurements of cloud, which uses emissivity-based cloud masking using BT and BTD
148 from multiple channels.

149 Figures 3a and 3b show scatter plots between MODIS cloud fractions and AirNow MDA8 ozone
150 and between NAQFC cloud fractions and MDA8 ozone, respectively, during August 1024 across
151 all reporting EPA AQS monitoring-sites. As the amount of UVA (ultraviolet radiation in 315-399
152 nm) strongly affects the ozone production by NO_2 photodissociation (e.g. j(NO2) in $\lambda < 420$ nm)
153 at the surface, it is evident that cloud fraction, and the eventual flux of photons reaching the
154 level of the surface, is a very dominant component determining ground-level ozone
155 concentration (Monks et al., 2004; Seinfeld and Pandis, 2006). Scatter plots in Figure 3a draw
156 data from more than 1000 sites across the CONUS under a variety of meteorological conditions
157 and precursor sources. Even with the high uncertainties here, we can see a notable separation

158 of ground-level ozone for each cloud-fraction bin, implying that photon flux is one of the most
159 dominant features determining tropospheric ozone photochemistry. Slope and offsets for line-
160 fitting MODIS CF versus AirNow MDA8 ozone are -11.33 and 49, respectively, implying that 10%
161 of CF change can cause around 1.13 ppb decrease in surface ozone. On the other hand, the
162 correlation between NAQFC CF and MDA8 ozone is slightly weaker (Figure 3b); slope and offsets
163 between NAQFC CF and MDA 8 ozone are -5.0 and 50.5, respectively, showing half as much
164 sensitivity in surface ozone according to the NAQFC CF compared to the MODIS CF.

165 Figures 3c and 3d are scatter plots for CF differences (NAQFC-MODIS) and MDA8 surface ozone
166 bias (NAQFC-AQS; left), and averaged O_3 biases for each 0.1 cloud-fraction bin (right). Since the
167 definition of cloud fraction in the model and the satellite are slightly different, we choose the
168 term "cloud fraction difference" instead of "cloud fraction bias." Slope of the linear regression is
169 -10.5 ppb/100% CF. The right-side panel shows averages of ozone biases for each 0.1 bin. The
170 vertical bars indicate 1 standard deviation. It is clear that where the model underestimates
171 cloud fraction, it likely overestimates surface ozone, although there are many intricacies of
172 tropospheric ozone chemistry involved.

173 Since Figure 3 shows data from all AQS sites, it includes multiple uncertainties from each site's
174 local characteristics, such as local emissions. We have conducted further investigation for
175 individual AQS sites to confirm if we can find similar MDA8 ozone to CF correlation. Figure 4
176 shows spatial distributions of each site's ozone to CF sensitivity (e.g., regression slope of MDA8
177 ozone and CF) and correlation coefficients during 5 months (May to September, 2014). MDA8
178 ozone decreases rapidly by the increase of CF in the southern regions, especially near the
179 coastal lines of Gulf of Mexico, such as Texas, Louisiana and Florida, up to -30 ppb/CF. In the
180 middle latitude regression slopes are around -10 ppb/CF, and some northern location areas
181 show positive correlation. Mean of total regression slope is -8.5 ppb/CF. Correlation coefficients
182 (R) also show stronger (negative) correlation in southern states, especially southeastern US up
183 to R=-0.7 while northeastern US shows much weaker correlation, implying accurate CF
184 information is important in southern US states.

185 **OZONE OVERPREDICTION** : As already described, current NAQFC cloud fields seem to have
186 fewer clouds than MODIS by 0.2. We have further estimated how this difference can affect the
187 general performance of surface ozone forecast. Previous studies address O_3 overpredictions of
188 global and regional chemical-transport models during the summer daytime over the eastern
189 United States (Chai et al., 2013; Eder et al., 2009; Fiore et al., 2009; Murazaki and Hess, 2006;
190 Nolte et al., 2008; Rasmussen et al., 2012; Reidmiller et al., 2009). Studies have addressed that
191 the vertical resolution (Murazaki and Hess, 2006), the coarse representation of emissions (Liang
192 and Jacobson, 2000), along with uncertainty in the heterogeneous reactions of aerosols (Martin
193 et al., 2003) contribute to the highly biased O_3 of the global chemical-transport models MOZART
194 or GEOS-Chem over the eastern United States. NAQFC also has a tendency to overestimate
195 surface ozone during ozone season. We may estimate the amount of possible overestimation of
196 surface ozone due to the underestimation of the cloud fraction and eventual overestimation of
197 photolysis rate. As the mean cloud fraction of model is 0.17 higher than the cloud-fraction
198 estimated from MODIS, by applying the -10.5 ppb/CF estimate, we can deduce that 1.8 ppb of
199 the surface-ozone overestimation is contributed from the underestimation of the cloud fraction.
200 Considering current NAQFC surface-ozone overestimation is around 5 ppb for the month of
201 August 2014, we can roughly suggest that almost 35% of this overestimation is due to faulty
202 estimation of the cloud field. Though this estimate is still very rough, this is definitely something

to consider carefully in order to improve the simulation of regional air quality and especially the simulation of surface ozone.

RESOLUTION ISSUE: In utilizing satellite-based cloud-fraction information, one concern is how to process data in terms of pixel resolution. As already mentioned, the cloud fraction is not a state variable; it is threshold- or retrieval-specific. For example, if we consider an area with 9 pixels with cloud fraction 0.6, fractional averaging of 9 cloud pixels should yield a 0.6 cloud fraction. However, if we first perform cloud masking for each pixel, we may have 9 cloud markings out of 9 pixels, resulting in 100% cloud fraction. This might not be a critical error on a global scale, but it is a crucial difference for regional or local scales intended for investigating the spatial scale of local ozone production. Since cloud fields are very localized phenomena, this information should be processed as finely as data are available.

To conclude, this study demonstrates that appropriate model of CF is crucial in the modeling of surface ozone chemistry. Further studies are needed in terms of the comparison of modeled- or satellite-based CF with actual surface level photon flux, as well as enhanced parameterization of CF in the air quality model.

4. REFERENCES

Bergman, J. W., and Salby, M. L. (1996). Diurnal variations of cloud cover and their relationship to climatological conditions. *Journal of Climate*, *9*(11), 2802–2820.

Byun, D., and Schere, K. L. (2006). Review of the Governing Equations, Computational Algorithms, and Other Components of the Models-3 Community Multiscale Air Quality (CMAQ) Modeling System. *Applied Mechanics Reviews*, *59*(2), 51. doi:10.1115/1.2128636

Byun, D. W., and Ching, J. K. S. (1999). *Science Algorithms of the EPA Models-3 Community Multiscale Air Quality (CMAQ) Modeling System*. Washington, DC, USA: US Environmental Protection Agency, Office of Research and Development.

Castro, T., Madronich, S., Rivale, S., Muhlia, A., & Mar, B. (2001). The influence of aerosols on photochemical smog in Mexico City. *Atmospheric Environment*, *35*(10), 1765–1772. doi:10.1016/S1352-2310(00)00449-0

Chai, T., Kim, H.-C., Lee, P., Tong, D., Pan, L., Tang, Y., Huang J., McQueen, J., Tsidulko, M., and Stajner, I. (2013). Evaluation of the United States National Air Quality Forecast Capability experimental real-time predictions in 2010 using Air Quality System ozone and NO_2 measurements. *Geoscientific Model Development*, *6*(5), 1831–1850. doi:10.5194/gmd-6-1831-2013

Dickerson, R. R., Kondragunta, S., Stenchikov, G., Civerolo, K. L., Doddridge, B. G., and Holben, B. N. (1997). The Impact of Aerosols on Solar Ultraviolet Radiation and Photochemical Smog. *Science*, *278*(5339), 827–830. doi:10.1126/science.278.5339.827

Eastman, R., and Warren, S. G. (2013). A 39-yr survey of cloud changes from land stations worldwide 1971-2009: Long-term trends, relation to aerosols, and expansion of the tropical belt. *Journal of Climate*, *26*(4), 1286–1303.

241 Eder, B., Kang, D., Mathur, R., Pleim, J., Yu, S., Otte, T., and Pouliot, G. (2009). A performance
242 evaluation of the National Air Quality Forecast Capability for the summer of 2007☆.
243 *Atmospheric Environment*, *43*(14), 2312–2320. doi:10.1016/j.atmosenv.2009.01.033

244 Fiore, a. M., Dentener, F. J., Wild, O., Cuvelier, C., Schultz, M. G., Hess, P., … Zuber, a. (2009).
245 Multimodel estimates of intercontinental source-receptor relationships for ozone pollution.
246 *Journal of Geophysical Research*, *114*(D4), 10816. doi:10.1029/2008JD010816

247 Geleyn, J. F., Hense, A., and Preuss, H. J. (1982). A comparison of model generated radiation
248 fields with satellite measurements. *Beitr. Phys. Atmos.*, *55*, 253–286.

249 He, S., and Carmichael, G. R. (1999). Sensitivity of photolysis rates and ozone production in the
250 troposphere to aerosol properties. *Journal of Geophysical Research*, *104*(D21), 26307.
251 doi:10.1029/1999JD900789

252 Jacobson, M. Z. (1998). Studying the effects of aerosols on vertical photolysis rate coefficient
253 and temperature profiles over an urban airshed. *J. of Geophys. Res.*, *103*(D9), 10593.
254 doi:10.1029/98JD00287

255 Kim, H., Ngan, F., Lee, P., and Tong, D. (2013). *Development of IDL-based geospatial data*
256 *processing framework for meteorology and air quality modeling*. Retrieved from
257 http://aqrp.ceer.utexas.edu/projectinfoFY12_13%5C12-TN2%5C12-TN2 Final Report.pdf

258 Lefer, B. L. (2003). Impact of clouds and aerosols on photolysis frequencies and photochemistry
259 during TRACE-P: 1. Analysis using radiative transfer and photochemical box models. *Journal*
260 *of Geophysical Research*, *108*(D21), 8821. doi:10.1029/2002JD003171

261 Liang, J., and Jacobson, M. Z. (2000). Effects of subgrid segregation on ozone production
262 efficiency in a chemical model. *Atmospheric Environment*, *34*(18), 2975–2982.
263 doi:10.1016/S1352-2310(99)00520-8

264 Madronich, S. (1987). Photodissociation in the atmosphere: 1. Actinic flux and the effects of
265 ground reflections and clouds. *Journal of Geophysical Research*, *92*(D8), 9740.
266 doi:10.1029/JD092iD08p09740

267 Martin, R. V., Jacob, D. J., and Yantosca, R. M. (2003). Global and regional decreases in
268 tropospheric oxidants from photochemical effects of aerosols. *Journal of Geophysical*
269 *Research*, *108*(D3), 4097. doi:10.1029/2002JD002622

270 Monks, P. S. (2004). Attenuation of spectral actinic flux and photolysis frequencies at the surface
271 through homogenous cloud fields. *Journal of Geophysical Research*, *109*(D17), D17206.
272 doi:10.1029/2003JD004076

273 Murazaki, K., and Hess, P. (2006). How does climate change contribute to surface ozone change
274 over the United States? *Journal of Geophysical Research*, *111*(D5), D05301.
275 doi:10.1029/2005JD005873

Nolte, C. G., Gilliland, A. B., Hogrefe, C., and Mickley, L. J. (2008). Linking global to regional models to assess future climate impacts on surface ozone levels in the United States. *Journal of Geophysical Research*, *113*(D14), D14307. doi:10.1029/2007JD008497

Otte, T. L., and Pleim, J. E. (2010). The Meteorology-Chemistry Interface Processor (MCIP) for the CMAQ modeling system: updates through MCIPv3.4.1. *Geoscientific Model Development*, *3*(1), 243–256. doi:10.5194/gmd-3-243-2010

Pour-Biazar, A., McNider, R. T., Roselle, S. J., Suggs, R., Jedlovec, G., Byun, D. W., … Cameron, R. (2007). Correcting photolysis rates on the basis of satellite observed clouds. *Journal of Geophysical Research*, *112*(D10), D10302. doi:10.1029/2006JD007422

Raga, G., Castro, T., and Baumgardner, D. (2001). The impact of megacity pollution on local climate and implications for the regional environment: Mexico City. *Atmospheric Environment*, *35*(10), 1805–1811. doi:10.1016/S1352-2310(00)00275-2

Rasmussen, D., Fiore, A., Naik, V., Horowitz, L. W., McGinnis, S. J., and Schultz, M. G. (2012). Surface ozone-temperature relationships in the eastern US: A monthly climatology for evaluating chemistry-climate models. *Atmospheric Environment*, *47*, 142–153. doi:10.1016/j.atmosenv.2011.11.021

Reidmiller, D. R., Fiore, a. M., Jaffe, D. a., Bergmann, D., Cuvelier, C., Dentener, F. J., … Zuber, A. (2009). The influence of foreign vs. North American emissions on surface ozone in the US. *Atmospheric Chemistry and Physics*, *9*(14), 5027–5042. doi:10.5194/acp-9-5027-2009

Schumann, U. (1989). Large-eddy simulation of turbulent diffusion with chemical reactions in the convective boundary layer. *Atmospheric Environment (1967)*, *23*(8), 6981. Retrieved from http://www.sciencedirect.com/science/article/pii/0004698189900565

Seinfeld, J. H., and Pandis, S. N. (2006). *Atmospheric Chemistry and Physics* (p. 1232).

Stephens, G. L. (2005). Cloud feedbacks in the climate system: A critical review. *Journal of Climate*.

Voulgarakis, A., Wild, O., Savage, N. H., Carver, G. D., and Pyle, J. A. (2009). Clouds, photolysis and regional tropospheric ozone budgets. *Atmospheric Chemistry and Physics*, *9*(21), 8235–8246. doi:10.5194/acp-9-8235-2009

Wild, O., Zhu, X., and Prather, M. (2000). Fast-J: Accurate simulation of in-and below-cloud photolysis in tropospheric chemical models. *Journal of Atmospheric Chemistry*, 2000. doi:10.1023/A:1006415919030

Wyngaard, J., and Brost, R. (1984). Top-down and bottom-up diffusion of a scalar in the convective boundary layer. *Journal of the Atmospheric Sciences*, *41*, 102–112. doi:http://dx.doi.org/10.1175/1520-0469(1984)041<0102:TDABUD>2.0.CO;2

311

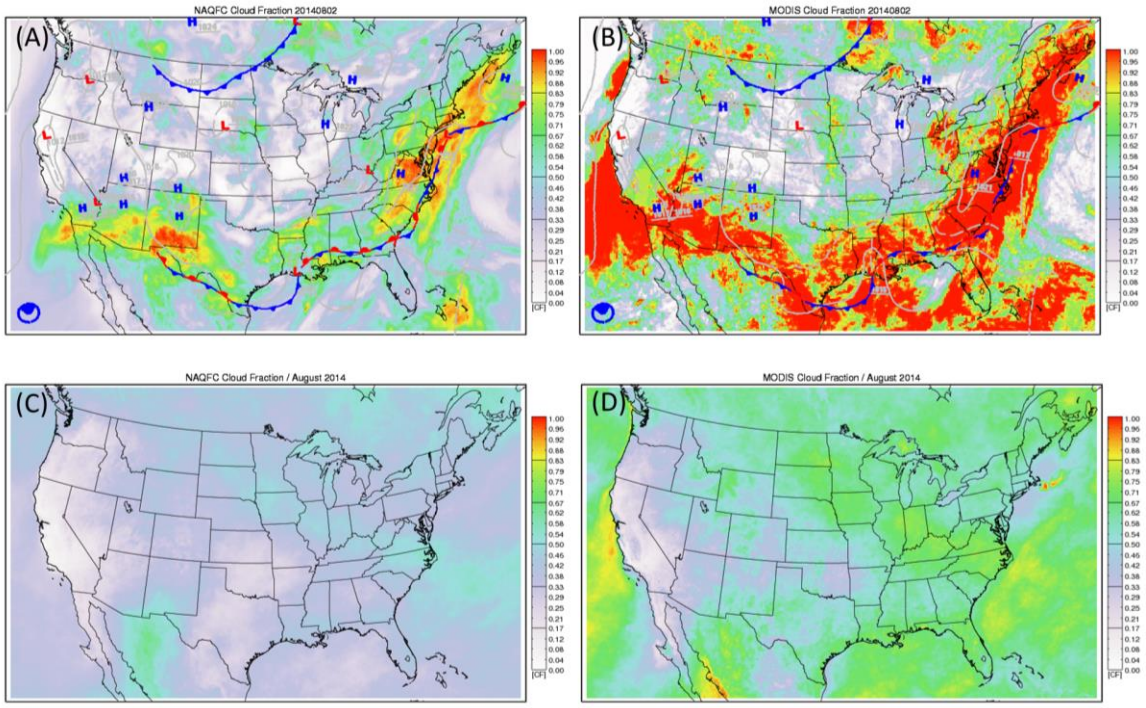

Figure 1. Spatial distributions of cloud fractions on Aug. 2, 2014 from NAQFC (a) and MODIS (b). NOAA NCEP surface weather chart at 18UTC is overlaid. Monthly averaged distributions are also shown for NAQFC (c) and MODIS (d).

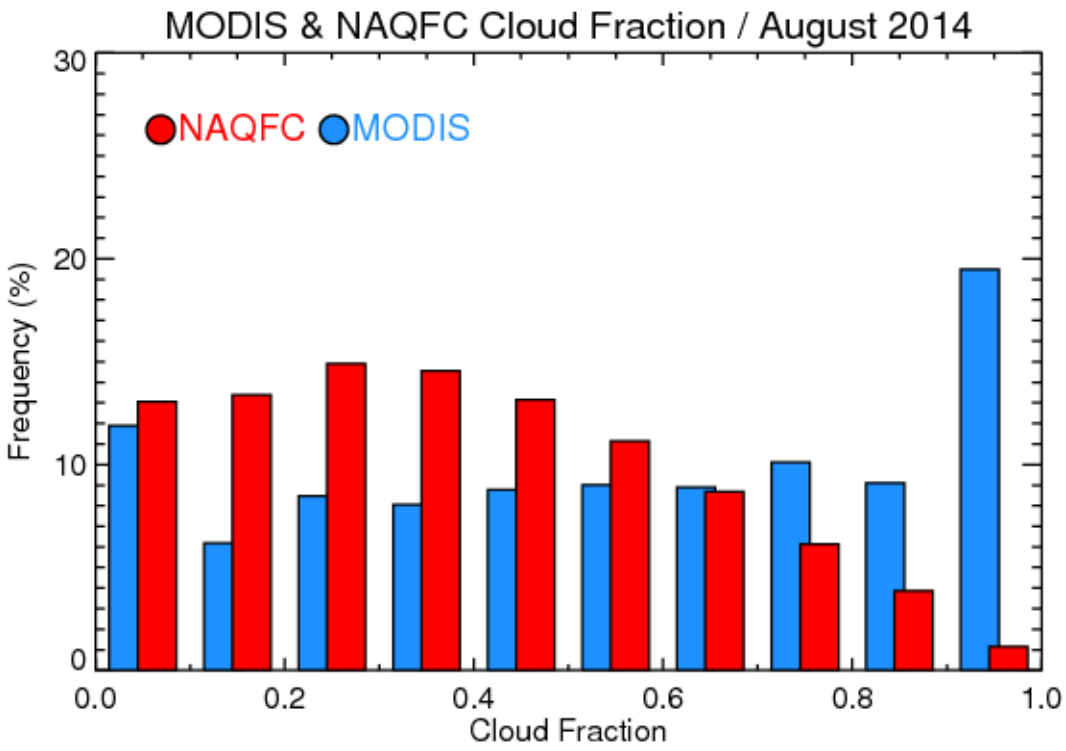

Figure 2. Occurrence frequency histogram for NAQFC cloud fractions (red) and MODIS cloud fractions (blue).

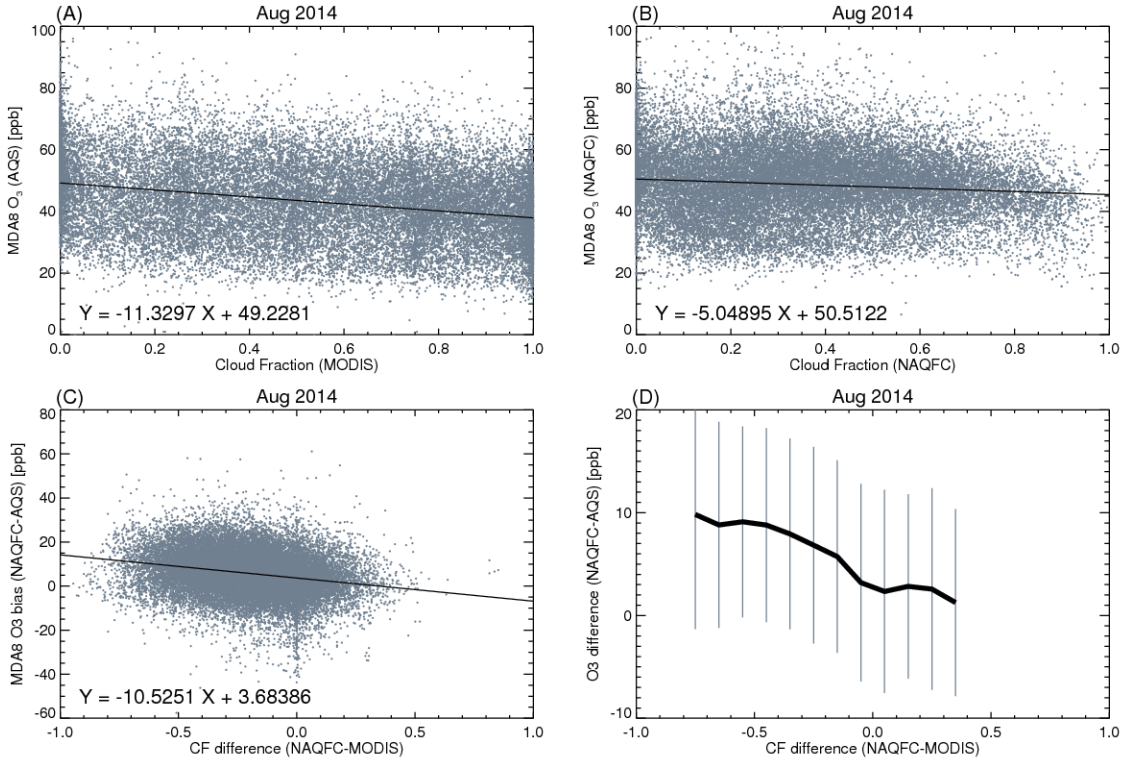

Figure 3. Scattered plots between MODIS cloud fractions and AQS MDA8 ozone (a), between NAQFC cloud fractions and MDA8 ozone (b), and between cloud fraction differences (NAQFC - MODIS) and MDA8 surface ozone bias (NAQFC-AQS) (c) during Aug. 2014 across 1024 AQS monitoring site locations. Averaged O_3 biases for each 0.1 cloud-fraction bin with 1 standard deviation (vertical bars) are also shown (d).

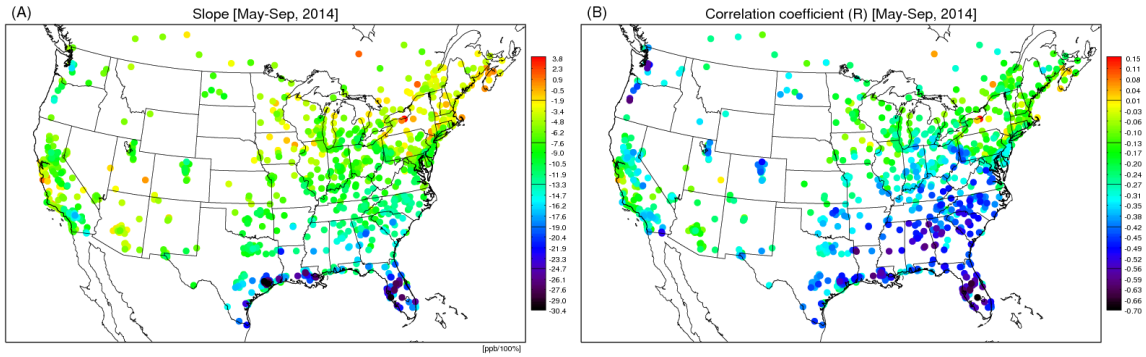

Figure 4. Spatial distributions of (a) slope and (b) correlation coefficient of linear regression between MODIS CF and MDA8 ozone.